

ANL/PHY/CP--80398

RECEIVED

NOV 22 1993

OSTI

## ELECTRON SCATTERING FROM POLARIZED DEUTERIUM AT VEPP-3

C. E. Jones, K. P. Coulter,<sup>a</sup> R. Gilman,<sup>b</sup> R. J. Holt,  
E. R. Kinney,<sup>c</sup> R. S. Kowalczyk, D. H. Potterveld, L. Young  
*Argonne National Laboratory, Argonne, Illinois USA*

V. V. Frolov, S. I. Mishnev, D. M. Nikolenko, S. G. Popov,  
I. A. Racheck, D. K. Toporkov, E. P. Tsentalovich, B. B. Wojtsekhowski,<sup>d</sup>  
*Budker Institute for Nuclear Physics, Novosibirsk, Russia*

C. W. de Jager, G. Retzlaff,<sup>e</sup> J. Theunissen, and H. de Vries  
*NIKHEF, Amsterdam, The Netherlands*

V. V. Nelyubin, V. V. Vikhrov  
*St. Petersburg Institute for Nuclear Physics, Gatchina, Russia*

V. N. Stibunov, A. V. Osipov  
*Tomsk Polytechnic Institute, Tomsk, Russia*

### Abstract

The experiment to measure the tensor analyzing power  $T_{20}$  of the deuteron using a tensor-polarized internal target at the VEPP-3 electron storage ring in Novosibirsk is currently in its second phase. Tensor-polarized deuterium atoms from an atomic beam source feed an active storage cell in the electron ring, serving as the target for a beam of 2 GeV unpolarized electrons. Analysis of the first Phase 2 data in the kinematic range  $Q^2 = 0.36 - 0.50 \text{ (GeV/c)}^2$  is reported here. Plans for the third phase of the experiment, which will use a high-density, laser-driven polarized deuterium target, are also discussed. The measurement of  $T_{20}$  from the second and third phases of the experiment will cover the kinematic region  $0.36 \leq q \leq 0.90 \text{ (GeV/c)}^2$  where  $T_{20}$  is particularly sensitive to isoscalar meson exchange currents.

### Overview

The electromagnetic structure of the deuteron is characterized by three form factors which can be measured in elastic electron-deuteron scattering;  $F_C$ , the charge monopole form factor,  $F_M$ , the magnetic form factor, and  $F_Q$ , the charge quadrupole form factor. Although the deuteron is a much-studied system, both in terms of experimental and theoretical studies, the models predict a wide range of values for the electromagnetic form factors even at modest momentum transfer. For example, see the papers presented in these proceedings alone [1]. Experimental data on polarization observables constrain models of the deuteron wave function, the effect of non-nucleonic degrees of freedom and the size of relativistic corrections. As data at higher momentum becomes available it is also possible to test calculations based upon quark degrees of freedom and ultimately to test QCD.

MASTER

Unpolarized scattering measurements are unable to fully separate the three form factors because the unpolarized cross section,

$$\left( \frac{d\sigma}{d\Omega} \right)_0 = \sigma_{Mott} (A(Q^2) + \tan^2(\theta/2)B(Q^2)), \quad (1)$$

depends upon two structure functions,

$$A(Q^2) = F_C^2 + (8\tau^2/9)F_Q^2 + (2\tau/3)F_M^2 \quad (2)$$

and

$$B(Q^2) = 4\tau(1+\tau)F_M^2/3, \quad (3)$$

where

$$\tau = Q^2/4m_d^2. \quad (4)$$

It is not possible to independently determine both  $F_C$  and  $F_Q$  without the introduction of polarization degrees of freedom into the scattering process. However, knowledge of both the unpolarized cross section and the tensor analyzing power  $T_{20}$  in elastic scattering of unpolarized electrons from tensor-polarized deuterium is sufficient to separate all three form factors. The expression for  $T_{20}$  in terms of the form factors is

$$T_{20} = -\sqrt{2}[x(x+2) + y/2]/[2(x^2 + y) + 1], \quad (5)$$

where

$$x = \frac{2}{3}\tau \left( \frac{F_Q}{F_C} \right) \quad (6)$$

and

$$y = \frac{\tau}{3}(1 + 2(1+\tau)\tan^2(\theta/2)) \left( \frac{F_M}{F_C} \right)^2. \quad (7)$$

In principle, a measurement of the tensor polarization of the outgoing deuterons in elastic scattering using unpolarized beam and target provides the same information about the structure of the deuteron, and this technique was employed in a recent measurement at Bates [2].

Above  $Q^2 \sim 0.40$  (GeV/c)<sup>2</sup> the tensor analyzing power  $T_{20}$  in elastic  $e - d$  scattering is very sensitive to the deuteron model used in the calculations because in the impulse approximation  $F_C$  is predicted to have a zero in this kinematic region and the position of the first minimum is quite sensitive to the introduction of isoscalar meson exchange currents [3]. Fig. 1 shows a plot of  $T_{20}$  calculated using a number of different theoretical models to show the range of the predictions. The dot-dash line is the calculation of Schiavilla and Riska using the Argonne V14 potential which includes meson exchange currents explicitly [3], the dotted line is the coupled channel calculation (model D') of Blunden et al. [4], the short dashed line is the relativistic calculation of Chung et al. using light-front dynamics to calculate the deuteron wave function from a nonrelativistic potential [5], and the solid line is the relativistic calculation of Hummel and Tjon using

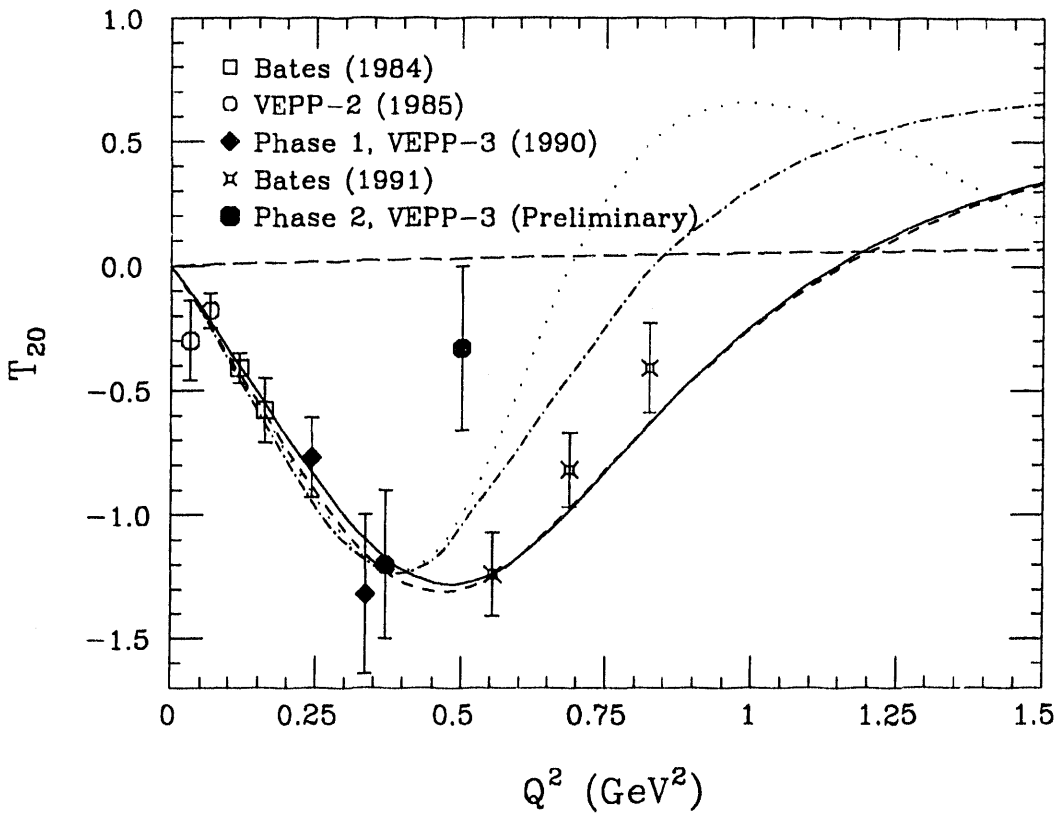


Fig. 1. Models of the tensor analyzing power in elastic  $e-d$  scattering  $T_{20}$ , calculated by Schiavilla and Riska (dotdash) [3], Blunden et al. (dot) [4], Chung et al. (short dash) [5], Hummel and Tjon (solid) [6], and Brodsky and Hiller (long dash) [7]. Also shown are data from previous measurements [2,8,9,10] and the preliminary analysis of the data from the ongoing internal target experiment at VEPP-3.

a covariant wave function calculated from the one-boson exchange model [6]. The long dashed line is a recent calculation based on perturbative QCD by Brodsky and Hiller [7]. Also shown are data from previous measurements [2,8,9,10].

Because the nucleon-nucleon model serves as input for “exact” calculations of the electromagnetic structure of the three-body system, one should be able to describe both the two and three-body systems starting from the same model of the deuteron. Fig. 2 shows the experimental data on the deuteron charge form factor and the three-body isoscalar charge form factor along with a consistent calculation for  $A = 2$  by Schiavilla and Riska [3] and for  $A = 3$  by Schiavilla, Pandharipande and Riska [11] performed both in the impulse approximation and with meson exchange currents. The inclusion of meson exchange currents shifts the minimum in  $F_C$  to lower momentum for both the two- and three-body system. A measurement of  $T_{20}$  in the range  $3.8 \leq q \leq 4.6 \text{ fm}^{-1}$  at the MIT-Bates electron accelerator using an unpolarized target and a recoil polarimeter [2] determined that the node in  $F_C$  lies at  $q = 4.39 \pm 0.16 \text{ fm}^{-1}$ , a value that is consistent with

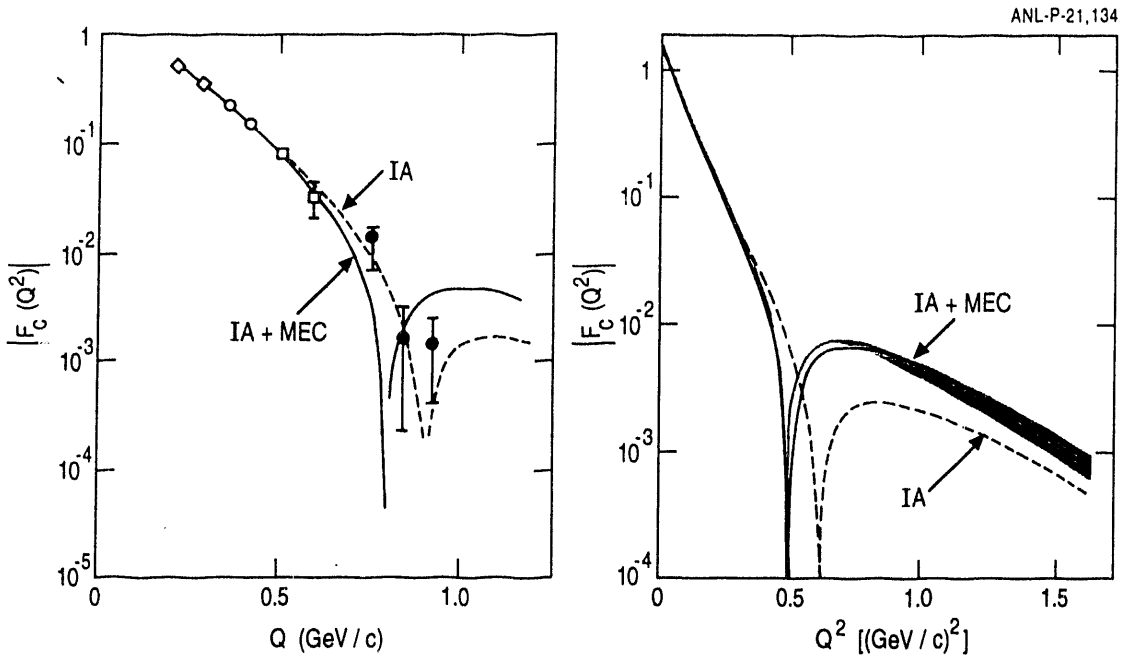


Fig. 2. The isoscalar charge form factor for the deuteron calculated by Schiavilla and Riska (left) [3] and for the three-body system calculated by Schiavilla, Pandharipande and Riska (right) [11] in the impulse approximation (dashed line) and including meson exchange currents (solid line). The experimentally-determined values of the  $A = 3$  isoscalar charge form factor are shown as a band to indicate the size of the experimental uncertainty [12].

impulse approximation calculations which include no meson exchange currents. However, the experimental data from the three-body system [12], shown as a light band to indicate the size of the experimental uncertainty, clearly indicate the necessity of including meson exchange currents. The shift to lower momentum of the minimum in  $F_C$  for the deuteron is a general feature of models that include meson exchange currents [13], and presently there is no model of the deuteron that both agrees with the deuteron experimental data and, when used as input for three-body calculations, successfully describes the existing data on the three-body isoscalar form factors. It is noted that relativistic corrections to the impulse approximation for the  $A = 3$  isoscalar charge form factor shift the minimum to higher momentum [14], worsening the agreement between theory and experiment and supporting the claim that meson exchange currents are important in the description of nuclear dynamics.

### The VEPP-3 Experiment

The experiment to measure  $T_{20}$  at the VEPP-3 electron storage ring at the Budker Institute for Nuclear Physics in Novosibirsk, Russia, has been underway since 1988, when the internal target technique was pioneered [15]. Results from Phase 1 have been reported [10], and the second phase of the experiment, which started in 1990, is ongoing. Installation

of Phase 3 is scheduled to begin in summer 1994. The experiment uses an internal tensor-polarized deuterium target and a beam of 2 GeV electrons.

The major difference between the different phases of the experiment is the type of target used. In the first phase an atomic beam source (ABS) coupled to a passive storage cell was used, with a resulting useful target thickness of  $3 \times 10^{11} \text{ cm}^{-2}$ . Currently the same ABS is coupled to an active storage cell which opens during beam filling and closes once the electrons are stored, providing a useful target thickness of  $2 \times 10^{12} \text{ cm}^{-2}$ . The third phase of the experiment will use a high density, laser-driven polarized deuterium source coupled to a passive storage cell. Flow rates of up to  $9 \times 10^{17} \text{ s}^{-1}$  have been demonstrated with the laser-driven source [16], so it is likely that the target thickness in Phase 3 will be limited by the vacuum requirements of the storage ring. Using the laser-driven source, a target thickness of  $\sim 4 \times 10^{14} \text{ cm}^{-2}$  is expected.

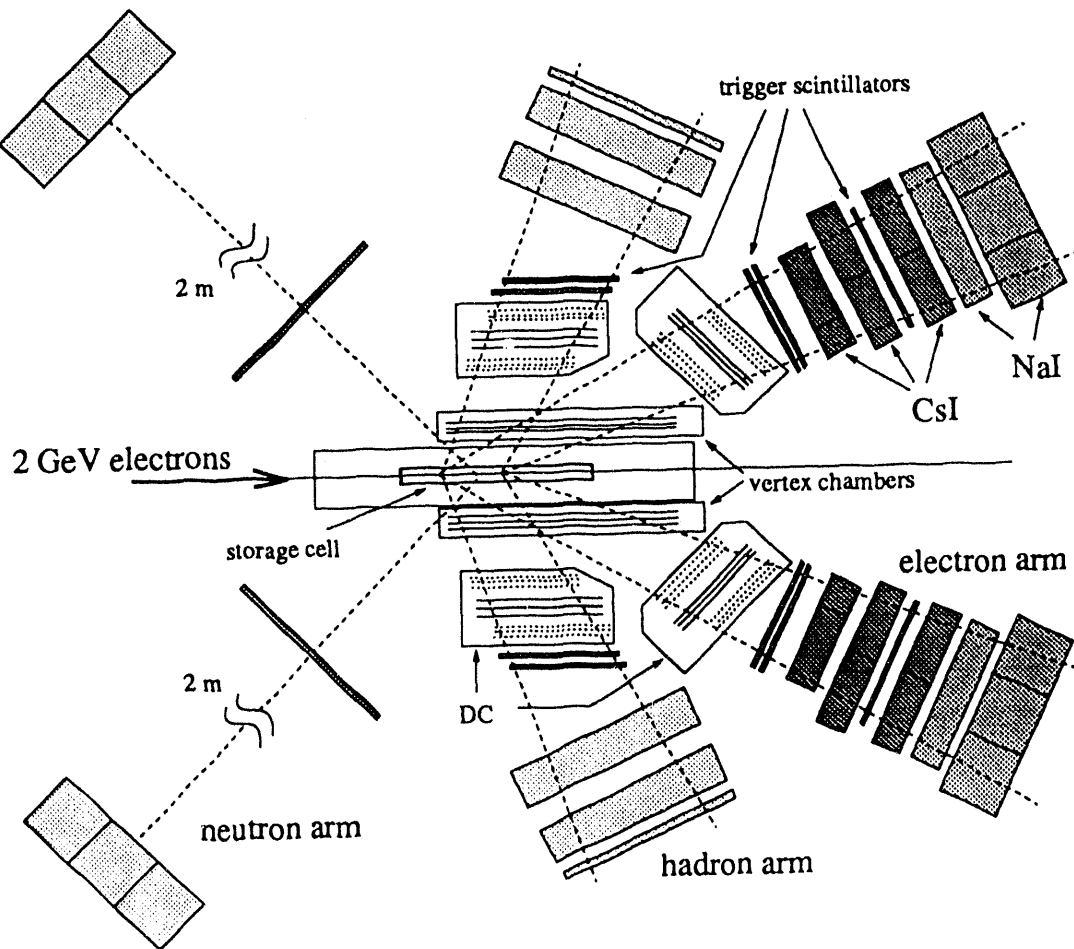


Fig. 3. Detector layout for Phase 2 and Phase 3 of the VEPP-3 experiment.

Fig. 3 shows the detector layout for the experiment. The detector system has two electron arms and two hadron arms arranged symmetrically around the electron beamline.

The arms are nearly identical and provide redundancy to minimize systematic errors. The electron arm covers the angular range  $20^\circ - 30^\circ$  and the hadron arm covers the range  $60^\circ - 70^\circ$ . Immediately outside the scattering chamber there are vertex chambers that record events for both the hadron and electron arms. The electron arm consists of drift chambers, thin scintillators for the event trigger, and a calorimeter that uses CsI and NaI blocks. The hadron arm has drift chambers, trigger scintillators, and thick scintillators for hadron detection. The system also contains two neutron arms consisting of thick scintillators in the backward direction ( $132^\circ - 138^\circ$ ) which are used in inelastic triggers. Not shown in Fig. 3 are small forward angle detectors installed at the end of the second data run which serve as a polarization monitor by measuring small angle  $e - d$  elastic scattering. Initially there was a high background in the detector because of beam halo scattering from the cell walls, however collimators installed in the beamline upstream of the interaction region effectively suppressed the background in the detectors, reducing the rate on the trigger scintillators of the electron and hadron arms approximately an order of magnitude.

The detector system used in Phase 1 was not optimized for an internal target, having been designed for an earlier experiment that used a gas jet target, so the effective target thickness seen by the detectors was only approximately a fifth of the total target. In the current experiment the detector system has been altered to view most of the central region of the target, so that the effective target thickness is half the total thickness. In the first run of Phase 2 the effective target thickness was  $(2.0 \pm 0.5) \times 10^{12} \text{ cm}^{-2}$ . Because the reliability of the active storage cell has proven problematic, a passive cell will be used during the next phase.

The layout of the target region is shown in Fig. 4. The polarized deuterium from an atomic beam source flows into a storage cell. Holding field magnets which provide a 900 Gauss holding field in the target region are placed outside the scattering chamber. Opposite the entrance to the storage cell is a small hole which allows atoms to pass into a Rabi polarimeter [17], so that the polarization of the beam from the ABS can be continuously monitored. The beam from the ABS has a tensor polarization of  $p_{zz} = \pm 0.98 \pm 0.05$ . Both the ABS and the polarimeter can be valved off from the beam line for maintenance.

### Results and Conclusions

In the current phase of the experiment two data runs have been taken and a third is planned. The results discussed here are from the preliminary analysis of the data from the first run only. The results are shown as the solid circles in Fig. 1. Because the extraction of  $T_{20}$  from the experimental asymmetry requires knowledge of the average  $p_{zz}$  of the atoms in the target cell, while the polarimeter measures the  $p_{zz}$  mainly of the atoms coming directly from the ABS, the average  $p_{zz}$  is determined by normalizing the data point at  $Q^2 = 0.37$   $(\text{GeV}/c)^2$  to the theoretical value calculated in the impulse approximation from the Paris potential. The normalization procedure yields  $p_{zz} = 0.67 \pm 0.19$ . The events constituting the two data points are simultaneously within the momentum acceptance of the detector system. The error bars on the higher momentum point include the systematic uncertainty from the normalization of the lower momentum datum. The value of  $p_{zz}$  extracted from the first data run by normalization is in agreement with a direct polarization measurement

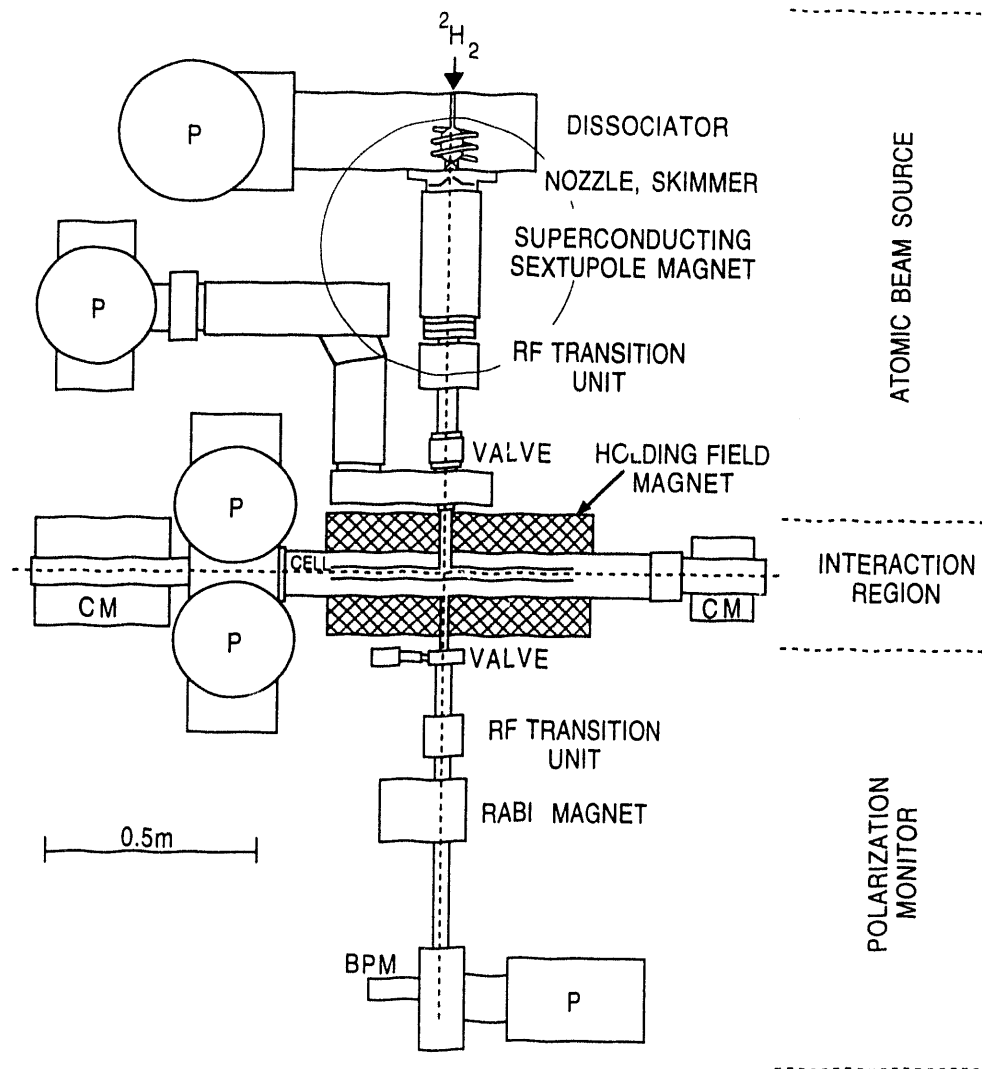


Fig. 4. Schematic of the target system, consisting of an atomic beam source coupled to a storage cell and a Rabi polarimeter. The vacuum pumps are denoted by 'P' and the compensating magnets by 'CM.'

using the small angle detectors installed at the end of the second data run, which gave a measured average of  $p_{zz} = 0.58 \pm 0.17$ .

With the data from the first run only, the statistical accuracy of this new datum at the higher momentum transfer is not sufficient to indicate the need for isoscalar meson exchange currents, although the point lies above the results of the previous measurement in this kinematic region. In view of the fact that the deuteron charge form factor extracted from the currently available data is incompatible with the calculations and experimental data for the  $A = 3$  system, it is necessary for experimentalists to verify the data while theorists improve their nuclear models. Because the polarized internal target technique is different from the recoil polarimeter technique used in the Bates measurement, the VEPP-

3 measurement will serve to experimentally verify the results from MIT-Bates using an experimental technique subject to different systematic errors. The improved statistics from the rest of the data from Phase 2 and from Phase 3 of the experiment, where a factor of 5 – 10 improvement in the figure of merit of the target is expected, will provide a stringent constraint theory in the region from  $0.4 \leq Q^2 \leq 0.9$  (GeV/c)<sup>2</sup> where isoscalar meson exchange currents significantly alter the analyzing power. Hopefully, a combination of new data and theory can rectify the existing discrepancy between descriptions of the two- and three-body systems.

### Acknowledgements

This work is supported in part by the U.S. Department of Energy, Nuclear Physics Division, under contract W-31-109-ENG-38.

### References

- <sup>a</sup> Current address: University of Michigan, Ann Arbor, Michigan, USA
- <sup>b</sup> Current address: Rutgers University, Piscataway, New Jersey, USA
- <sup>c</sup> Current address: University of Colorado, Boulder, Colorado, USA
- <sup>d</sup> Current address: Rensselaer Polytechnic Institute, Troy, New York, USA
- <sup>e</sup> Current address: Saskatchewan Accelerator Laboratory, Saskatoon, Canada
- <sup>1</sup> See, for example, the contribution of P. U. Sauer and of S. J. Wallace.
- <sup>2</sup> I. The *et al.*, Phys. Rev. Lett. **67**, 173 (1991).
- <sup>3</sup> R. Schiavilla and D. O. Riska, Phys. Rev. C **43**, 437 (1991).
- <sup>4</sup> P. G. Blunden *et al.*, Phys. Rev. C **40**, 1541 (1989).
- <sup>5</sup> P. L. Chung *et al.*, Phys. Rev. C **37**, 2000 (1988).
- <sup>6</sup> E. Hurnmel and J. A. Tjon, Phys. Rev. Lett. **63**, 1788 (1989).
- <sup>7</sup> Stanley J. Brodsky and John R. Hiller, Phys. Rev. D **46**, 2141 (1992).
- <sup>8</sup> M. E. Schulze *et al.*, Phys. Rev. Lett. **52**, 597 (1984).
- <sup>9</sup> V. F. Dmitriev *et al.*, Phys. Lett. **157B**, 143 (1985).
- <sup>10</sup> R. Gilman *et al.*, Phys. Rev. Lett. **65**, 1733 (1990).
- <sup>11</sup> R. Schiavilla, V. R. Pandharipande, and D. O. Riska, Phys. Rev. C **41**, 309 (1990).
- <sup>12</sup> A. Amroun *et al.*, Phys. Rev. Lett. **69**, 253 (1992).
- <sup>13</sup> H. Henning, J. Adams, Jr., P. U. Sauer, and A. Stadler, submitted to Phys. Rev. C.
- <sup>14</sup> George Rupp and J. A. Tjon, Phys. Rev. C **45**, 2133 (1992).
- <sup>15</sup> R. Gilman *et al.*, Nucl. Instrum. Meth. **A327**, 277 (1993).
- <sup>16</sup> M. Poelker *et al.*, ANL Preprint Phy-7140-ME-93.
- <sup>17</sup> A. V. Evstigneev, S. G. Popov, and D. K. Toporkov, Nucl. Instrum. Meth. **A238**, 12 (1985).

### DISCLAIMER

This report was prepared as an account of work sponsored by an agency of the United States Government. Neither the United States Government nor any agency thereof, nor any of their employees, makes any warranty, express or implied, or assumes any legal liability or responsibility for the accuracy, completeness, or usefulness of any information, apparatus, product, or process disclosed, or represents that its use would not infringe privately owned rights. Reference herein to any specific commercial product, process, or service by trade name, trademark, manufacturer, or otherwise does not necessarily constitute or imply its endorsement, recommendation, or favoring by the United States Government or any agency thereof. The views and opinions of authors expressed herein do not necessarily state or reflect those of the United States Government or any agency thereof.

# END

DATE  
FILMED

1/12/94

